PNAS RESEARCH ARTICLE | IMMUNOLOGY AND INFLAMMATION

Raver1 links *Ripk1* RNA splicing to caspase-8-mediated pyroptotic cell death, inflammation, and pathogen resistance

Boyao Zhang[a,1], Pontus Orning[a,b,1], Jesse W. Lehman[c], Alexandre Dinis[a], Leslie Torres-Ulloa[c], Roland Elling[d,e], Michelle A. Kelliher[f], John Bertin[g,h], Megan K. Proulx[i], Jon D. Goguen[i], Liv Ryan[b], Richard K. Kandasamy[a,b,j], Terje Espevik[b,k], Athma A. Pai[c], Katherine A. Fitzgerald[a,b,l,2], and Egil Lien[a,b,2]

Affiliations are included on p. 11.

Contributed by Katherine A. Fitzgerald; received October 15, 2024; accepted January 8, 2025; reviewed by Clare E. Bryant and Jonathan C. Kagan

Multiple cell death and inflammatory signaling pathways converge on two critical factors: receptor-interacting serine/threonine kinase 1 (RIPK1) and caspase-8. Careful regulation of these molecules is critical to control apoptosis, pyroptosis, and inflammation. Here, we found a pivotal role of Raver1 as an essential regulator of *Ripk1* pre-mRNA splicing, expression, and functionality and the subsequent caspase-8-dependent inflammatory cell death. We show that Raver1 influences mRNA diversity primarily by repressing alternative exon inclusion. Macrophages from *Raver1*-deficient mice exhibit altered splicing of *Ripk1*. As a result, *Raver1*-deficient primary macrophages display diminished cell death and decreased interleukin-18 and interleukin-1ß production, when infected with *Yersinia* bacteria, or by restraining TGF-ß-activated kinase 1 or IKKβ in the presence of lipopolysaccharide, tumor necrosis factor family members, or interferon-γ. These responses are accompanied by reduced activation of caspase-8, Gasdermin D and E, and caspase-1 in the absence of *Raver1*. Consequently, *Raver1*-deficient mice showed heightened susceptibility to *Yersinia* infection. Raver1 and RIPK1 also controlled the expression and function of the C-type lectin receptor Mincle. Our study underscores the critical regulatory role of Raver1 in modulating innate immune responses and highlights its significance in directing in vivo and in vitro inflammatory processes.

RIPK1 | caspase-8 | gasdermin | pyroptosis | IL-1ß

Significance

Caspase-8 and the kinase receptor-interacting serine/threonine kinase 1 (RIPK1) are critical focal points for several inflammation and cell death pathways and, thus, require careful regulation. We identified the RNA splicing factor Raver1 as a critical factor directing the splicing of *Ripk1* to modulate RIPK1/caspase-8-driven pyroptosis, apoptosis, and inflammation. Raver1 is central for macrophage responses to *Yersinia* bacteria, initiated after blockade of kinases TGF-ß-activated kinase 1 (TAK1) and IκB kinase complex (IKK), measured as activation of RIPK1, caspase-8, Gasdermin D, caspase-3, interleukin-1ß (IL-1β), and interleukin-18 (IL-18). Importantly, Raver1 is necessary for host resistance to *Yersinia* infection in vivo. We propose that Raver1 is key for correct tuning of RIPK1-caspase-8-dependent processes.

Cell death and inflammatory pathways frequently share signaling mechanisms critical for inflammation during microbial infection or tissue injury. Receptor-interacting serine/threonine kinase 1 (RIPK1) is a key regulator in both inflammatory pathways and apoptosis, pyroptosis, and necroptosis. RIPK1 is engaged upstream of caspase-8 activation during extrinsic apoptotic cascades and is required for optimal nuclear factor-kappa-B (NF-κB) signaling after lipopolysaccharide (LPS) or tumor necrosis factor (TNF) stimulation (1, 2). Therefore, RIPK1 and caspase-8 are integral mediators governing innate immune signaling processes in inflammation and antimicrobial host defenses. RIPK1 is tightly regulated via posttranslational modifications (3). Additional mechanisms likely influence RIPK1-caspase-8-dependent pathways. Further investigations into these intricate regulatory mechanisms are crucial to understanding the pathophysiology of many inflammatory conditions to develop targeted therapeutic interventions.

Essential information on the interconnectivity between cell death and inflammatory pathways has come from studies using *Yersinia* bacteria as a model system. Human-pathogenic *Yersinia* include *Yersinia pestis*, the causative agent of plague, and the gastrointestinal pathogens *Yersinia pseudotuberculosis* and *Yersinia enterocolitica*. During *Yersinia* infection, the bacterial Type III secretion system effector YopJ (or YopP in *Y. enterocolitica*) inhibits TGF-ß-activated kinase 1 (TAK1), the IκB kinase complex (IKKα/ß), and mitogen-activated protein kinases through acetylation of phosphorylation sites (4–7). Both TAK1 (8, 9) and IKKα/β (10, 11) are essential to restrain RIPK1-driven cytotoxicity and inflammatory pathologies via inhibitory phosphorylation of RIPK1. Thus, *Yersinia* infection unleashes RIPK1 kinase activity and the subsequent assembly of cytosolic cell death complex II, involving RIPK1, Fas-associated death domain protein (FADD), and caspase-8 (1, 2, 12, 13). This pathway licenses apoptosis by activating caspase-8 (13, 14). We and others have recently presented evidence for the crosstalk between apoptotic and pyroptotic pathways. In immune cells, *Yersinia*-activated caspase-8 also cleaves Gasdermin D (GSDMD), initiating atypical pyroptosis and allowing the release of proinflammatory cytokines interleukin-1ß (IL-1ß) and interleukin-18 (IL-18) (2, 15–17), as well as inducing secondary caspase-1 cleavage (13–15), which further amplifies inflammation.

Reviewers: C.E.B., University of Cambridge; and J.C.K., Boston Children's Hospital.

Competing interest statement: P.O. is an employee of Immunity Bio. J.B. is an employee of Sanofi. K.A.F. is a founder of Danger Bio, a Related Sciences company, and a member of the scientific advisory board for Related Sciences, Generation Bio, and Janssen. None of the work in this study is related to any of these activities.

[1]B.Z. and P.O. contributed equally to this work.

[2]To whom correspondence may be addressed. Email: Kate.Fitzgerald@umassmed.edu or Egil.Lien@umassmed.edu.

This article contains supporting information online at https://www.pnas.org/lookup/suppl/doi:10.1073/pnas.2420802122/-/DCSupplemental.

Published February 13, 2025.

Yersinia-triggered RIPK1-caspase-8-dependent cell death is characterized by a complex interplay between components of apoptosis and pyroptosis. The effect of YopJ can also be mimicked by treatment with LPS or TNF combined with pharmacological inhibition of TAK1 (TAK1-i) or IKK (IKK-i), whereas the impact of interferon-γ (IFNγ) in the context of TAK1 blockade is unclear. YopJ-induced cell death is independent of caspase-1, whereas the caspase-8-dependent release of IL-1ß is partially influenced by caspase-8-controlled caspase-1 activation (15). Loss of *Gsdmd* delays cell death upon blockade of TAK1 or IKKα/ß and reduces IL-1ß and IL-18 secretion (15, 17).

Using a CRISPR-based screen combined with *Yersinia* infection, we identified Raver1 as a regulator of RIPK1-caspase-8 signaling by influencing pre-mRNA splicing of *Ripk1*. Loss of *Raver1* promotes the inclusion of an alternative *Ripk1* exon, resulting in the production of a truncated dysfunctional neopeptide and reduced overall RIPK1 levels. *Raver1*-deficient macrophages and neutrophils display impaired responses to *Yersinia* or LPS/TNF/IFNγ+TAK1-blockade-induced pyroptosis, and IL-1ß/IL-18 release. Importantly, compromised antimicrobial responses culminated in the decreased ability of *Raver1*-deficient animals to resist *Yersinia* challenge. We also extend these findings and establish that Raver1 regulates C-type lectin receptor (CLR) Mincle (*Clec4e*) expression and signaling via its effects on RIPK1. Together, our study defines a critical role for Raver1 in regulating innate immune responses, emphasizing its importance in orchestrating inflammatory processes both in vitro and in vivo.

Results

A CRISPR Screen in Primary Macrophages Identifies Raver1 as a Regulator of *Yersinia*-Induced RIPK1-Caspase-8-Mediated Cell Death. To identify regulators of RIPK1-caspase-8-mediated signaling, we performed an unbiased genome-wide CRISPR-Cas9 cell death screen using primary mouse bone marrow–derived macrophages (BMDM) infected with *Yersinia*. To better focus on the caspase-8 signaling component, Cas9-expressing *Ripk3*$^{-/-}$ bone marrow cells were transduced with a genome-wide single-guide RNA (sgRNA) library and differentiated into macrophages. Once progenitor cells were fully differentiated, cells were infected with *Y. pestis*. DNA from the surviving populations was isolated, and enriched sgRNAs were identified. The screen identified several known components, including RIPK1, GSDMD, and caspase-8, as well as components of the lysosomal Rag–Ragulator complex (Fig. 1*A*), recently described as important regulators of RIPK1-caspase-8 activation (18). In addition, top hits included two proteins involved in alternative splicing: Raver1 and Ptbp1 (Fig. 1*A*). Raver1 and Ptbp1 are both implicated in pre-mRNA splicing regulation, including alternative splicing of α-tropomyosin exon 3 in smooth muscle cells (19–21). Raver1 is proposed to cooperate with Ptbp1, the latter exerts a broad influence on a wide range of splicing events (22), and its deletion is associated with embryonic mortality in mice. The specific contribution of Raver1 to innate immune function in vivo and in vitro, however, remains largely unexplored. Thus, we focused additional analysis on the newly identified hit—Raver1.

We first confirmed the effect of Raver1 by transducing Cas9 transgenic primary BMDMs with sgRNAs targeting *Raver1*. Compared to control cells transduced with nontargeting sgRNAs, cells lacking *Raver1* were protected from cell death induced by *Yersinia* infection or by mimicking *Yersinia* infection using the combined action of LPS plus TAK1-i (Fig. 1*B* and *SI Appendix*, Fig. S1*A*). This inhibition was specific to RIPK1-caspase-8-induced death as cells lacking *Raver1* responded normally to NLRC4-caspase-1-mediated pyroptosis induced in response to *Salmonella enterica* serovar Typhimurium (Fig. 1*B*) (23).

To determine the role of Raver1 in innate immunity, we generated mice lacking *Raver1* via CRISPR/Cas9. This yielded a line (#6) with a 171 bp deletion in exon 1 of the *Raver1* gene which led to a loss of any detectable protein expression (*SI Appendix*, Fig. S1 *B–D*). Unlike *Ptbp1*$^{-/-}$ mice that are embryonically lethal, *Raver1*$^{-/-}$ mice are viable and healthy throughout life expectancy. BMDMs from these mice recapitulated protection from *Yersinia*- or chemical-mimetic-induced cytotoxicity found in sg*Raver1*-transduced cells (Fig. 1*C*).

Raver1 Represses Alternative Splicing of *Ripk1* to Maintain RIPK1 Protein Abundance. Given the proposed role of Raver1 in regulating alternative splicing, we sought to determine how the loss of *Raver1* reshapes the transcriptome and contributes to *Yersinia*-induced cytotoxicity. We performed differential splicing analyses on RNA-seq datasets in untreated BMDMs from *Raver1*$^{-/-}$ vs. WT mice, revealing pervasive global changes in transcriptome composition (Fig. 1*D* and *SI Appendix*, Fig. S1*D*). Of the 1,773 significant alternative splicing events, 745 were skipped exon events, and there was a strong bias toward skipped exon inclusion in *Raver1*$^{-/-}$ BMDMs (Fig. 1*D* and *SI Appendix*, Fig. S1*E*). Together, these data indicate that Raver1 is important for repressing exon inclusion during pre-mRNA splicing.

Strikingly, a *Ripk1* alternative exon shows the most significant skipped exon change upon *Raver1* deletion (Fig. 1*E*). Indeed, *Ripk1* was the only member of the caspase-8 signaling pathway with significant Raver1-mediated splicing events. Thus, these analyses identified *Ripk1* as a potential splicing target of Raver1 in primary macrophages, whose dysregulation in the absence of *Raver1* might modulate *Yersinia*-induced cytotoxicity. Interestingly, Ptbp1 was proposed as a regulator of necroptosis in a fibroblast cell line by impacting *Ripk1* alternative splicing (24); another cell death screen also suggested the involvement of Raver1 (25). Therefore, we hypothesized that Raver1 functions in caspase-8-mediated innate immune responses by modulating the splicing of *Ripk1* in primary cells.

An in-depth investigation on *Ripk1* splicing patterns in BMDMs validated our findings that loss of *Raver1* altered *Ripk1* transcript composition, through increased inclusion of the *Ripk1* alternative exon between exons 4 and 5 (Fig. 1*F* and *SI Appendix*, Fig. S1*F*), causing a frameshift that introduced an early stop codon. We predicted this would result in a truncated RIPK1 isoform variant with a protein neosequence at the C-terminus, that we called Splice I (Fig. 1*G*). Although Splice I shares sequences with the majority of the RIPK1 kinase domain, it lacks a key portion of it—phosphorylation site Ser166, as well as crucial domains, including intermediate, RIP homotypic interaction motif, and death domains.

We designed qPCR assays quantifying *Ripk1* canonical exons 4 to 5, full-length *Ripk1* (exemplified by exon 9), and the inclusion of the *Ripk1* alternative exon (exon 4-alt. exon), linked to the production of Splice I. We found that *Raver1*$^{-/-}$ BMDMs had a five-fold increase in Splice I expression, as measured by the inclusion of the alternative exon, compared to WT BMDMs, resulting in ~50% reduction in full-length *Ripk1* transcripts (Fig. 1 *H* and *I* and *SI Appendix*, Fig. S1*G*). Accordingly, full-length RIPK1 protein was reduced >60% in the absence of *Raver1* (Fig. 1*J* and *SI Appendix*, Fig. S1*H*). This reduction can potentially be attributed to nonsense-mediated decay of transcripts harboring the premature stop codon. Of note, the RIPK1 antibody recognizes the C-terminus of the protein and cannot detect the splice variant. In contrast to RIPK1, *Raver1*$^{-/-}$ macrophages or *Raver1* sgRNA-treated

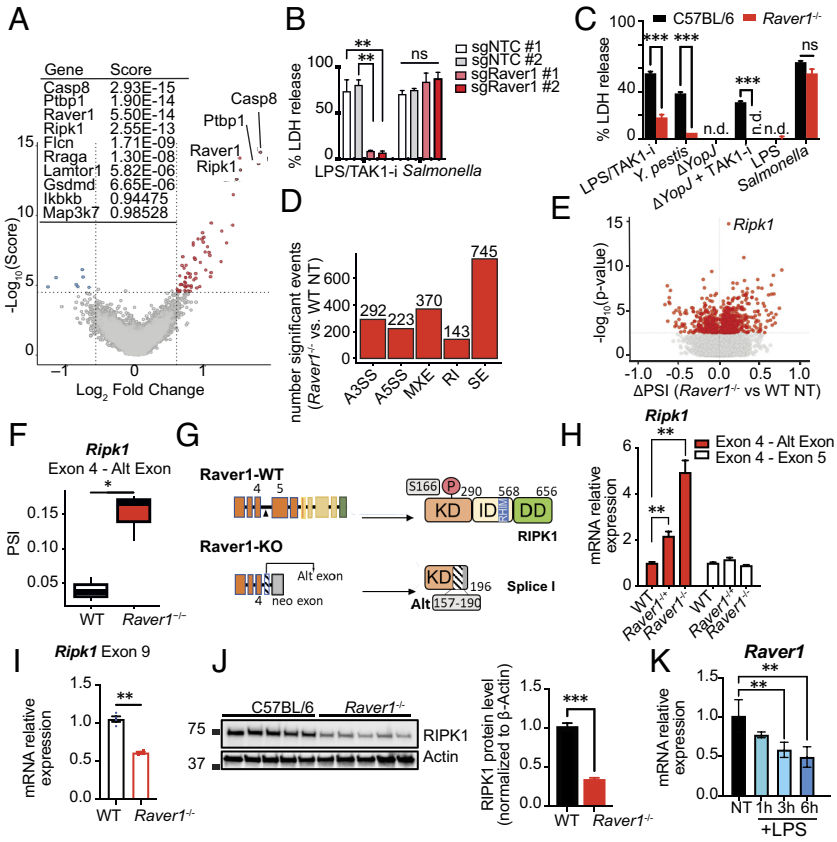

Fig. 1. Raver1 regulates RIPK1 RNA splicing and signaling. (*A*) A CRISPR screen was performed in Cas9-expressing *Ripk3*$^{-/-}$ BMDMs infected with *Y. pestis*. Log_2-fold change and MAGeCK Robust Rank Aggregation enrichment scores are shown to indicate the essentiality of the genes. (*B* and *C*) Cas9-expressing BMDMs transduced with *Raver1*-targeting sgRNAs or a nontargeting control (NTC) (*B*) or *Raver1*$^{-/-}$ BMDMs (*C*) were challenged with *Y. pestis*, *Y. pestis* △YopJ (△YopJ) or LPS and TAK1-i, or *Salmonella*. Cell death was measured by lactate dehydrogenase (LDH) release after 4 h. (*D–F*) Differential splicing analysis on *Raver1*$^{-/-}$ and WT BMDMs using RNA-seq data (three biological replicates each). (*D*) Frequencies of significant alternative splicing events in *Raver1*$^{-/-}$ vs. WT BMDMs. A3SS, alternative 3′ splice sites; A5SS, alternative 5′ splice sites; MXE, mutually exclusive exons; RI, retained intron; SE, skipped exons (*E*) Skipped exon event differences between *Raver1*$^{-/-}$ vs. WT were depicted, with percent spliced-in (ΔPSI) and $-\log_{10}$(*P*-value) shown. *Ripk1* is highlighted as the most significant SE change upon *Raver1* deletion. (*F*) PSI of *Ripk1* alternative exon 4 inclusion. (*G*) Model for canonical and alternative splicing of *Ripk1* in the presence or absence of *Raver1*. Kinase domain (KD), intermediate domain (ID), RIP homotypic interaction motif (RHIM), death domain (DD). (*H* and *I*) qPCR of mRNA levels of *Ripk1* exons in indicated resting BMDMs. (*J*) Protein levels of RIPK1 in WT or *Raver1*$^{-/-}$ BMDMs from five mice; the right-hand side shows quantification from the Western blot. (*K*) qPCR of *Raver1* mRNA levels in C57BL/6 BMDMs treated with LPS for the indicated times. Data are presented as the mean ± SD (*B*, *C*, and *K*) or ± SEM (*H–J*) for triplicates from three or more independent experiments. (*H–K*) Data normalized to β-Actin. For comparison between two groups, Student's *t* test was used; for more than two groups, ANOVA with the Bonferroni post hoc test was used. ns, not significant; **P* ≤ 0.05; ***P* ≤ 0.01; ****P* ≤ 0.001. Abbreviations: n.d., not detected; NT, nontreated; Alt exon, alternative exon.

cells had comparable protein levels of caspase-8, TAK1, FADD, and RIPK3 (*SI Appendix*, Fig. S1 *H* and *I*).

Expression of *Raver1* decreased with time following stimulation with LPS in macrophages (Fig. 1*K*). This could potentially indicate the presence of a feedback loop that could limit excessive inflammation to achieve homeostasis following pathway activation, although the dynamic regulation and the nature of relevant transcripts require further investigation.

Raver1 Is Required for RIPK1-Caspase-8-Mediated Cell Death in Primary Phagocytes. To examine how Raver1 mediates cell death, we infected WT and *Raver1*$^{-/-}$ cells with *Yersinia*. BMDMs from *Raver1*$^{-/-}$ mice were significantly protected from pyroptosis induced by human-pathogenic *Yersinia* spp. (*Y. pestis, Y. pseudotuberculosis, Y. enterocolitica*) (Fig. 2*A*), while maintaining a normal response to *Salmonella* (Fig. 2*B*). Additionally, BMDMs from *Raver1*$^{-/-}$ mice were protected from pyroptosis following treatments that mimic *Yersinia* infection, including TAK1 or IKK inhibitors in combination with LPS, TNF, or its family member lymphotoxin-α (LT-α) (Fig. 2 *B–D* and *SI Appendix*, Fig. S2 *A* and *B*). Macrophages from a second *Raver1*-deficient mouse line (#4) (*SI Appendix*, Fig. S1 *B* and *C*) had a similar phenotype (*SI Appendix*, Fig. S2*C*). The delayed death in *Raver1*$^{-/-}$ BMDMs was also seen in peritoneal macrophages (*SI Appendix*, Fig. S2*D*). Recent studies have revealed that in neutrophils, RIPK1 regulates pyroptosis and IL-1 release through caspase-8-dependent activation of Gasdermin E (GSDME) during *Yersinia* infection (26). Interestingly, we observed attenuated cell death in *Raver1*$^{-/-}$ neutrophils following TNF+TAK1-i treatment (Fig. 2*E*), indicating a broader role of Raver1 in different immune cells involved in innate immunity. Deleting MLKL did not further protect against cell death induced by TNF or LPS plus TAK1-i in *Raver1*-deficient macrophages (*SI Appendix*, Fig. S2*E*), suggesting that no secondary activation of the necroptosis pathway was occurring following this pyroptotic/apoptotic response.

In macrophages, caspase-8 cleaves GSDMD into a pore-forming p30 N-terminal fragment to trigger pyroptosis, and subsequent caspase-3 activation contributes to additional processing to a p22 fragment (15). *Raver1*$^{-/-}$ BMDMs displayed reduced caspase-8 and GSDMD processing in response to *Yersinia* spp. in a YopJ/YopP-dependent manner (Fig. 2*F*). Furthermore, activation of GSDMD and caspase-8 was also compromised in *Raver1*$^{-/-}$ macrophages when the infection was mimicked by TNF, LT-α, or LPS plus TAK1-i treatment (Fig. 2*G* and *SI Appendix*, Fig. S2

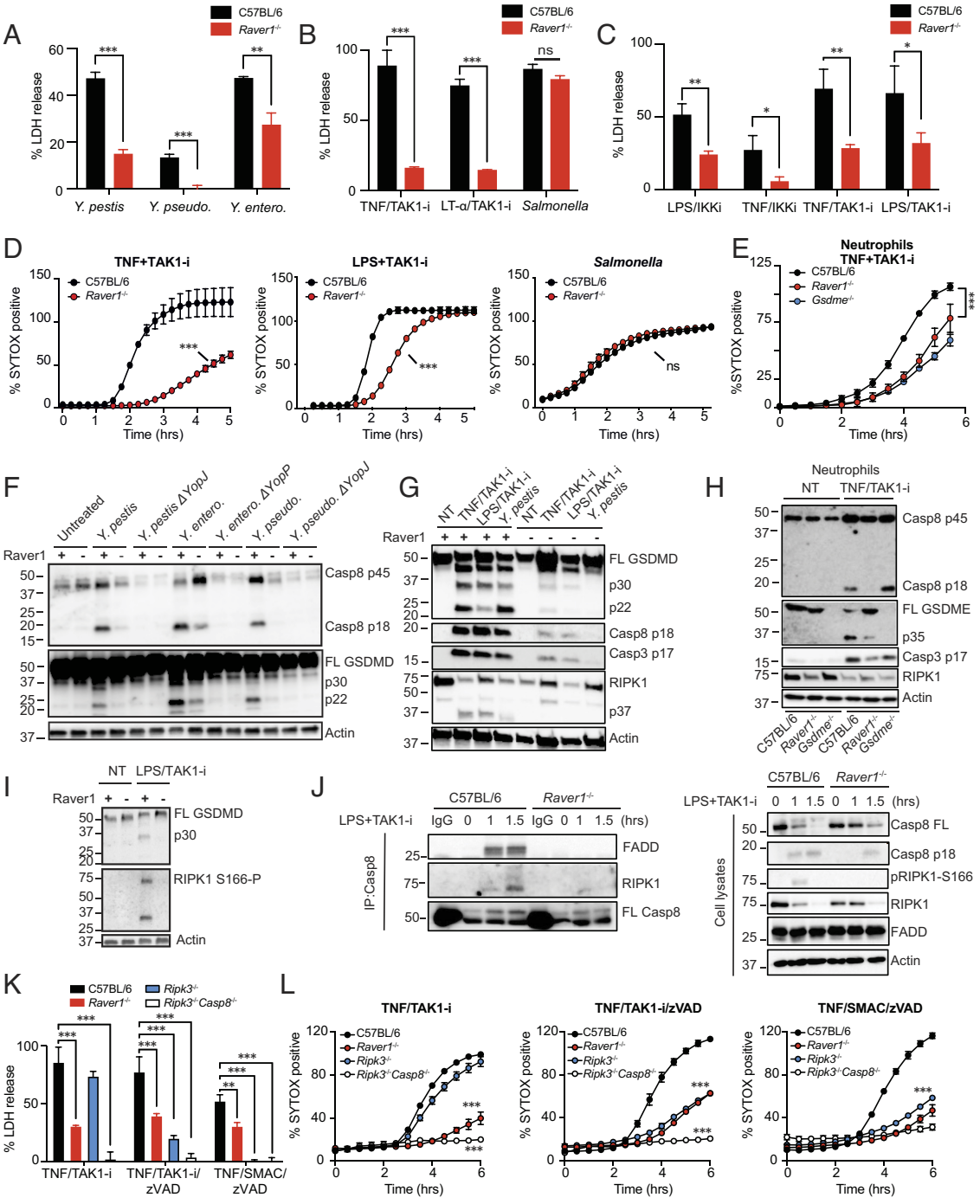

Fig. 2. *Raver1*-deficient macrophages and neutrophils are resistant to pyroptotic cell death and activation of RIPK1, caspase-8, and GSDMD/E after *Yersinia* challenge. (*A–E*) C57BL/6 or *Raver1*$^{-/-}$ BMDMs (*A–D*) or neutrophils (*E*) were challenged with *Yersinia* spp., *Salmonella*, TAK1-i or IKK-i plus LPS, TNF, or LT-α. Cell death was measured by LDH release after 4 h (*A–C*) or SYTOX membrane permeability assay (*D* and *E*). (*F–I*) Cell lysates from BMDMs (*F*, *G*, and *I*) or neutrophils (*H*) from indicated mice were analyzed by immunoblotting for GSDMD/E, caspase-8, caspase-3, and RIPK1 after 2 to 3 h (*F–H*) or 1 h (*I*). (*J*) Caspase-8 immunoprecipitation (IP: Casp8) or cell lysates of C57BL/6 or *Raver1*$^{-/-}$ BMDMs treated with LPS+TAK1-i for indicated timepoints were analyzed by immunoblotting on FADD, RIPK1, and caspase-8. (*K* and *L*) Indicated BMDMs were stimulated with TNF, TAK1-i, or a SMAC mimetic ± pan-caspase inhibitor zVAD-fmk pretreatment and then analyzed for LDH release after 4 h (*K*) or SYTOX assay (*L*). Data are presented as the mean ± SD for triplicate wells from three or more independent experiments. Immunoblots are representative of ≥3 performed. For comparison between two groups, Student's *t* test was used; for more than two groups, ANOVA with Bonferroni post hoc test was used. n.s., not significant; *$P \le 0.05$, **$P \le 0.01$, ***$P \le 0.001$. Abbreviations: FL, full-length; +, *Raver1*$^{+/+}$; −, *Raver1*$^{-/-}$ (*F*, *G*, and *I*).

F and *G*). Thus, the protection from cell death observed in *Raver1*$^{-/-}$ BMDMs was due to reduced processing and activation of caspase-8 and GSDMD.

We next examined other proteins downstream of caspase-8 and observed blunted processing of RIPK1, caspase-3, and GSDME in *Raver1*-deficient macrophages and neutrophils (Fig. 2 *G* and *H* and *SI Appendix*, Fig. S2*H*), events all correlating with diminished RIPK1-caspase-8-mediated cell death. This aligns with a recent study proposing that RIPK1 regulates GSDMD and GSDME processing in macrophages and neutrophils (26). Moreover, *Raver1*$^{-/-}$ cells did not show any detectable phosphorylation of RIPK1 S166, after TAK1-blockade with LPS or TNF family members (Fig. 2*I* and *SI Appendix*, Fig. S2*G*), suggesting RIPK1 activation is greatly suppressed in the absence of *Raver1*. This aligns with the proposed model of Splice I lacking the RIPK1 S166 activation site, a key autophosphorylation residue (27). In *Raver1*$^{-/-}$ cells, limited

RIPK1-caspase-8 association was detected following LPS+TAK1 inhibition (Fig. 2*J*), indicating that formation of cell death complex II is defective in *Raver1*-deficient BMDMs. This likely reflects a reduction of the critical complex component, RIPK1. Together, this information points toward a model in which Raver1 regulates RIPK1 upstream of RIPK1-caspase-8 death complex assembly, likely by balancing the levels of full-length RIPK1 and the Splice I variant.

RIPK1 kinase is also required for controlling RIPK3-MLKL-dependent necroptosis upon caspase inhibition (28). Similar to *Ripk3*$^{-/-}$ BMDMs, deletion of *Raver1* significantly decreased susceptibility to necroptosis induced by pan-caspase inhibitor zVAD-FMK in addition to TNF and TAK1-i or SMAC mimetic (Fig. 2 *K* and *L*). This is consistent with a previous observation that CRISPR-RNA-mediated knock-out of *Ptbp1* downregulates necroptosis in fibroblast cells (24). Altogether, the above evidence demonstrates that Raver1 is indispensable for RIPK1-caspase-8-mediated pyroptosis/apoptosis as well as RIPK1-RIPK3-mediated necroptosis.

Raver1-Deficient Primary Phagocytes Display Impaired Inflammatory Responses. Our prior work indicated that this RIPK1-caspase-8-GSDMD pathway is directly involved in *Yersinia*-induced release of IL-1ß and IL-18, and these proinflammatory cytokines are important for host resistance to *Yersinia* strains (13, 15, 29–31). Reduced RIPK1-caspase-8-dependent release of IL-1ß was observed in *Raver1*$^{-/-}$ macrophages and *Raver1*$^{-/-}$ neutrophils following *Yersinia* infection, or TNF/LPS plus TAK1 or IKK inhibition (Fig. 3 *A–D* and *SI Appendix*, Fig. S3 *A–C*). This reduction in IL-1ß correlated with reduced activation of caspase-8 and GSDMD/E in *Raver1*$^{-/-}$ cells (Fig. 2 *F–I* and *SI Appendix*, Fig. S2 *F–H*). And the maturation and cleavage of IL-1ß, but not the generation of pro-IL-1ß, is dramatically reduced in the absence of Raver1 (Fig. 3*D*).

Inhibition and deletion of TAK1 (8, 15) or IKKβ (32, 33) is associated with IL-1β release and ASC-NLRP3 inflammasome activity. We previously suggested that ASC-NLRP3 functions downstream of caspase-8 and potassium efflux in these stimulatory conditions (15). Consequently, caspase-1 p20 cleavage and ASC inflammasome oligomerization were also abrogated in *Raver1*$^{-/-}$ macrophages (Fig. 3 *E* and *F* and *SI Appendix*, Fig. S3*D*). Furthermore, our data suggest that the absence of *Raver1* in BMDMs does not directly influence IL-1ß secretion induced by other inflammasome ligands that trigger activation of caspase-1-dependent inflammasomes: NLRP3 (Pam3CSK4+ATP or nigericin), NLRC4 (*Salmonella*), Pyrin (Pam3CSK4+TcdB toxin and *Y. pestis* ΔYopMΔYopJ), and AIM2 (Pam3CSK4 + poly[dA:dT]) (*SI Appendix*, Fig. S3 *E* and *F*). Taken together, Raver1 controls RIPK1-caspase-8-dependent release of IL-1ß and secondary ASC inflammasome activation, contributing to inflammation.

Another key cytokine for immune responses and antimicrobial defenses is IFNγ. IFNγ levels are elevated during bacterial and viral infections, including *Yersinia* and SARS-CoV-2 (29, 34). Less is known about cytotoxicity involving IFNγ, but recent evidence has implicated IFNγ in inducing RIPK1-caspase-8-mediated cell death and inflammation during the cytokine storm and multiorgan failure following SARS-CoV-2 challenge (34). Furthermore, IFNγ+LPS stimulation also engages caspase-8 (35), whereas the role of RIPK1 in this condition is unclear. Strikingly, our experiments showed that IFNγ+TAK1-i also induced considerable cell death in WT BMDMs (Fig. 3*G* and *SI Appendix*, Fig. S4 *A* and *B*). In contrast, *Raver1*$^{-/-}$ macrophages were protected against IFNγ+TAK1-i-induced cytotoxicity (Fig. 3*H* and *SI Appendix*, Fig. S4 *C* and *D*) with a concomitant reduction in caspase-8, GSDMD, GSDME, and caspase-3 activation (Fig. 3*I* and *SI Appendix*, Fig. S4 *E* and *F*). The cell death was controlled by RIPK1, GSDMD, and caspase-8 (Fig. 3*H* and *SI Appendix*, Fig. S4 *C* and *G*). IFNγ+TAK1-i stimulation appeared fundamentally different from IFNγ+LPS in that the latter condition did not involve RIPK1 kinase activity or Raver1 (*SI Appendix*, Fig. S4*G*).

IL-18 is an IFNγ-inducing factor, and both cytokines play critical roles in host defenses during *Yersinia* infection (29, 31). We found that IFNγ+TAK1-i induces the release of a substantial amount of IL-18 protein in a Raver1-dependent manner, similar to *Yersinia* infection, or TAK1-i plus LPS or TNF (Fig. 3*J*). In contrast, Raver1 did not influence IL-18 induced by *Salmonella* (Fig. 3*J*), consistent with the lack of impact of Raver1 on *Salmonella*-triggered IL-1ß and cell death (Figs. 2 and 3).

To determine how inflammation impacts IFNγ-induced cell death, we examined TNFR1 signaling. We reported a partial role for TNFR1 in *Yersinia*- or LPS+TAK1-i-induced macrophage death (15), we now observed that IFNγ+TAK1-i-induced cytotoxicity was heavily influenced by TNF signaling, as the absence of TNFR1 reduced cell death to background levels (Fig. 3 *K* and *L*). These data suggest that TAK1 activity restrains IFNγ-induced cell death and inflammation via secondary TNF release and TNFR1 signaling, mediated by Raver1-regulated RIPK1 and caspase-8.

The Splice I Variant Interacts with RIPK1 to Negatively Regulate Cell Death. To further explore the role of TNF and confirm the role of Raver1 and RIPK1 splice variants in a different system, we used Cas9-expressing WEHI164-clone13 fibrosarcoma cells, a highly TNF-sensitive cell line that has been used in a death-based bioassay for TNF activity (36). We observed that these cells underwent RIPK1 and caspase-mediated cell death following treatment with TNF or TNF+TAK1-i, which was abolished by deletion of *Raver1* (Fig. 4*A* and *SI Appendix*, Fig. S5*A*). These effects were conserved in human cells, as sgRNAs against *Raver1* also reduced TNF+TAK1-i-induced cell death mediated by RIPK1/Caspase-8 in human U2OS osteosarcoma cells (Fig. 4*B* and *SI Appendix*, Fig. S5 *B* and *C*).

To study the function of the RIPK1 Splice I variant (Fig. 1*G*), we ectopically expressed FLAG-tagged Splice I in HEK293T cells, and this resulted in the production of a 22 kDa peptide (Fig. 4*C*), indicating Splice I can be translated into protein. Splice I interacts with full-length RIPK1, as evidenced by the detection of HA-tagged RIPK1 from immunoprecipitates of FLAG-Splice I when coexpressed (Fig. 4*D*). This was accompanied by reduced expression and activation of newly synthesized RIPK1 (HA-tagged) (Fig. 4 *C* and *D*). However, we did not observe a reduction in preexisting RIPK1 protein utilizing a doxycycline-induced Splice I system (*SI Appendix*, Fig. S5*D*). This suggests that increased expression of Splice I negatively affects RIPK1 protein synthesis. The reduced RIPK1 levels could be a key aspect in the downregulation of signaling.

The Splice I variant was unable to drive cytotoxicity alone but reduced RIPK1-induced cytotoxicity (Fig. 4 *E* and *F*). Data in Fig. 5*A* indicated that WEHI164 cells could be suitable for testing Splice I function. Ectopic expression of the RIPK1 Splice I product in WEHI164-clone13 cells reduced TNF-induced cell death (Fig. 4*G*). These results could be explained by a dominant-negative action of Splice I binding to full-length RIPK1 and, consequently, reduced ability of RIPK1 to induce cell death. Taken together, these findings suggest that Raver1 regulates RIPK1-caspase-8-mediated cell death and inflammation through alternative splicing of *Ripk1*. Loss of *Raver1* reduced full-length RIPK1 levels and increased expression of a dysfunctional truncated Splice I variant that bound

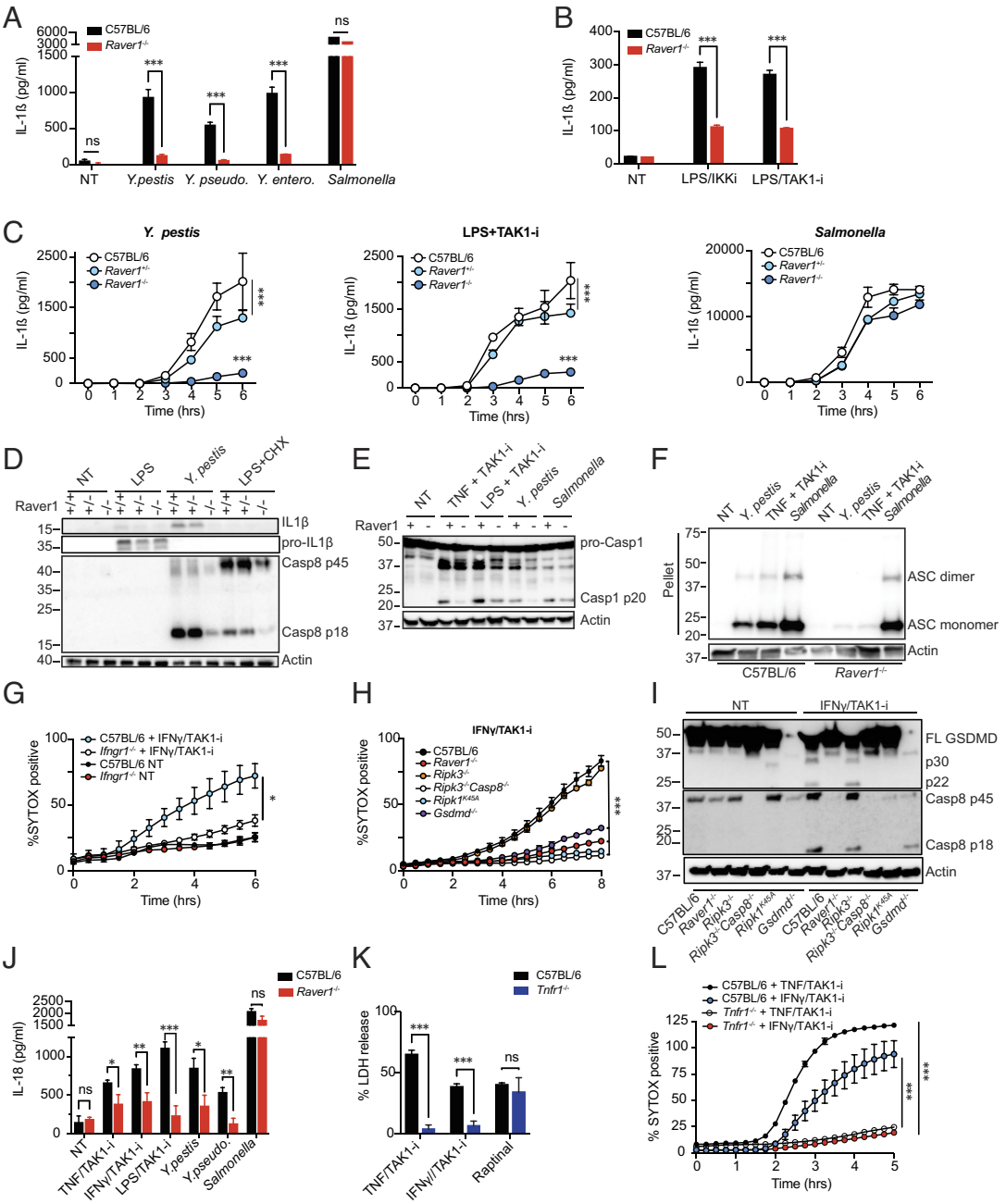

Fig. 3. Raver1 controls TAK1-restrained IL-1β/IL-18 release and IFNγ-driven inflammatory responses. (*A–C*) C57BL/6 or *Raver1*$^{-/-}$ BMDMs were treated with *Yersinia* spp., *Salmonella*, or LPS with TAK1-i or IKK-i. IL-1β release into the supernatant as measured by the Enzyme-linked immunosorbent assay (ELISA) after 5 h or at the indicated time points. (*D* and *E*) Cell lysates plus supernatants were analyzed by immunoblotting for caspase-1, -8, or IL-1β cleavage 3 h after the indicated stimulation. (*F*) Oligomerization of ASC in the inflammasome-enriched and crosslinked lysates as detected by immunoblotting. (*G–I*) BMDMs of indicated genotypes were treated with IFNγ plus TAK1-i. Cell death was measured by SYTOX assay (*G* and *H*). GSDMD and caspase-8 processing at 3 h were detected by immunoblotting (*I*). (*J*) IL-18 levels as measured by the ELISA on supernatants from C57BL/6 or *Raver1*$^{-/-}$ BMDMs challenged with indicated bacteria or TAK1-i for 5 h. (*K* and *L*) C57BL/6 or *Tnfr1*$^{-/-}$ BMDMs were treated with TAK1-i plus TNF or IFNγ, or Raptinal alone. Cell death was measured by LDH release after 4.5 h (*K*) or SYTOX assay (*L*). Data are presented as the mean ± SD for triplicates from three or more independent experiments. Immunoblots are representative of three immunoblots performed. For comparison between two groups, Student's *t* test was used; for more than two groups, ANOVA with Bonferroni post hoc test was used. n.s., not significant; *$P \le 0.05$, **$P \le 0.01$, ***$P \le 0.001$. Abbreviations: CHX, cycloheximide.

to RIPK1 and inhibited its ability to induce cell death. Collectively, these events have profound effects on normal RIPK1 function.

Raver1 Cooperates with Ptbp1 to Regulate *Ripk1* Splicing and Cell Death. Raver1 has been proposed as a Ptbp1 cofactor in regulating alternative splicing events but may also function independently of Ptbp1 (20, 37). Both Raver1 and Ptbp1 ranked high on our CRISPR screen (Fig. 1*A*), and deletion of either by CRISPR/Cas9 was associated with increased inclusion of the *Ripk1* alternative exon and diminished cytotoxicity in Cas9-BMDMs treated with LPS/TAK1-i (Fig. 5*A* and *SI Appendix*, Figs. S1*A* and S6 *A* and *B*). These data suggested that both Raver1 and Ptbp1 could influence exon exclusion in *Ripk1*. To test the cooperative effects of the two splicing factors, we transfected WT or *Raver1*$^{-/-}$ macrophages with siRNA against *Ptbp1* (*SI Appendix*, Fig. S6*C*). *Ptbp1* knockdown by siRNA further protected *Raver1*$^{-/-}$ immortalized macrophages from TNF/LPS+TAK1-i-induced cytotoxicity (Fig. 5*B* and *SI Appendix*, Fig. S6*D*). Furthermore, the inclusion of the *Ripk1* alternative exon is further increased in this condition, compared to either deletion of *Raver1* or knockdown of *Ptbp1* (Fig. 5*C*). Consistently, the level

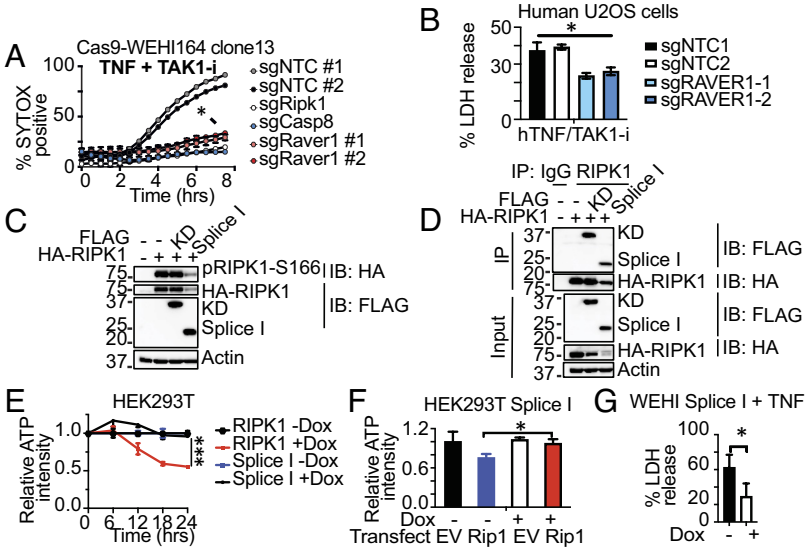

Fig. 4. Raver1 dysfunction results in a RIPK1 splicing isoform, Splice I, that negatively regulates cell death. (*A* and *B*) WEHI164 clone 13 fibrosarcoma cells (*A*) or human U2OS osteosarcoma cells (*B*) transduced with indicated sgRNAs were treated with TNF and TAK1-i. Cell death was measured by SYTOX assay (*A*) or LDH release after 10 h (*B*). (*C* and *D*) HEK293T cells were cotransfected with vectors encoding RIPK1-HA and RIPK1 variants (Splice I-Flag or RIPK1-kinase domain [KD]-Flag) or empty pcDNA3 for 24 h and analyzed by immunoblotting (*C*), or immunoprecipitation with RIPK1 antibodies followed by Flag or HA immunoblotting (*D*). (*E*) Doxycycline (Dox)-induced RIPK1 or RIPK1-Splice I was expressed in HEK293T cells. Cell death was measured by reduced ATP intensity after Dox treatment for the indicated times. (*F*) HEK293T cells expressing Dox-induced RIPK1-Splice I were transfected with RIPK1 or empty vector (EV) 12 h post-Dox addition, and cell death was measured by reduced ATP intensity after another 12 h. (*G*) WEHI164 clone 13 cells expressing Dox-induced RIPK1-Splice I were stimulated with TNF (50 ng/mL) 12 h post-Dox addition, and cell death was assessed by LDH release after 10 h. Data are presented as the mean ± SD for triplicates from three or more independent experiments. Immunoblots are representative of three immunoblots performed. For comparison between two groups, Student's *t* test was used; for more than two groups, ANOVA with Bonferroni post hoc test was used. ns, not significant; $*P \le 0.05$, $***P \le 0.001$. Abbreviations: NTC, nontargeting control; hTNF, human TNF.

of canonically spliced *Ripk1* mRNA was reduced (Fig. 5*D*) upon targeting both splicing factors, resulting in lower protein levels of full-length RIPK1 than in *Raver1*$^{-/-}$ macrophages or *Ptbp1* knockdown alone (Fig. 5*E*). Together, these data suggest that Raver1 cooperates with Ptbp1 to regulate *Ripk1* pre-mRNA splicing and cell death signaling.

Identification of Additional Innate Immune Signals Regulated by Raver1. We performed a broad transcriptome analysis to explore whether Raver1 regulates the expression of genes other than RIPK1. RNA-seq data indicated that *Ripk1* read counts were reduced, and the expression of only a small number of genes was influenced by the absence of *Raver1* in macrophages (Fig. 6*A* and *SI Appendix*, Fig. S7*A*). The majority of the innate immunity pathways tested appeared largely preserved in *Raver1*$^{-/-}$ BMDMs (*SI Appendix*, Fig. S7*A*). For example, only nonsignificant differences were observed in LPS- and TNF-induced NF-κB activation (*SI Appendix*, Fig. S7 *B–D*). Notable exceptions were polyI:C-TLR3 (*SI Appendix*, Fig. S7 *E* and *F*) and ssRNA encephalomyocarditis virus (EMCV)-MDA5 (*SI Appendix*, Fig. S7*F*); responses to both these stimulants were reduced in *Raver1*$^{-/-}$ BMDMs. This is consistent with a potential contribution of RIPK1, as previous work demonstrates that TLR3 drives the association of RIPK1 with TIR-domain-containing adapter inducing IFNβ (TRIF) (38). Prior work also implicated Raver1 in regulating MDA5 signaling (39), which is triggered by EMCV (40). In additional experiments, LPS or polyI:C both transcriptionally induced IFN-ß mRNA, and we found this gene to be substantially less induced in *Raver1*-deficient macrophages compared to wild-type cells. This supports a hypothesis of gene-specific impact of Raver1 on transcription, with a possible emphasis on TRIF-mediated responses, as polyI:C is completely dependent upon TRIF (*SI Appendix*, Fig. S7*G*). Notably, both LPS and polyI:C induced cell death in BMDM when combined with TAK1-i, and both stimulations were dependent upon Raver1 and TRIF (*SI Appendix*, Fig. S7*H*) (13, 15).

RNA-seq analysis also identified macrophage *Cd4* mRNA as being downregulated and potentially influenced by Raver1 (*SI Appendix*, Fig. S7*A*); however, further analysis revealed no significant differences in CD4 protein expression levels and CD4^{+} T cell composition in spleens from *Raver1*$^{-/-}$ mice (*SI Appendix*, Fig. S7 *I* and *J*). The composition of other spleen lymphoid and myeloid populations was also similar in the absence of *Raver1* (*SI Appendix*, Fig. S7*J*), indicating that immune cell composition is largely preserved in *Raver1*$^{-/-}$ animals.

Raver1 Regulates Mincle-Dependent TNF Release via RIPK1. One of the few genes with reduced baseline gene expression in the absence of *Raver1* (*SI Appendix*, Fig. S7*A*) was *Clec4e* (encoding Mincle). Mincle is a CLR that plays a pivotal role in recognizing various pathogens and damaged cells. It initiates NF-κB activation via CARD9 and is susceptible to upregulation by TNF (41, 42). Subsequent analysis indicated a sharp reduction in Mincle-*Clec4e* mRNA (Fig. 6*B*) and protein expression (Fig. 6*C*), as well as cellular responses in *Raver1*$^{-/-}$ BMDMs to two Mincle ligands: synthetic mycobacterial cord factor, trehalose-6,6′-dibehenate (TDB) (43), and cell-death-associated ß-glucosylceramide (44) (Fig. 6 *D–G*). However, we did not observe significant differences in alternative splicing events for *Clec4e* in the absence of *Raver1* (*SI Appendix*, Fig. S8 *A* and *B*); thus, the contribution of Raver1 on Mincle-*Clec4e* gene expression could be indirect. One connection between Mincle and Raver1 could be linked to the capacity of RIPK1 to modulate CLR signaling through CARD9 (45). Notably, using RIPK1-K45A kinase-dead mutant BMDMs, we found a marked reduction in TDB-induced TNF and IL-1ß transcription and release (Fig. 6 *F* and *G* and *SI Appendix*,

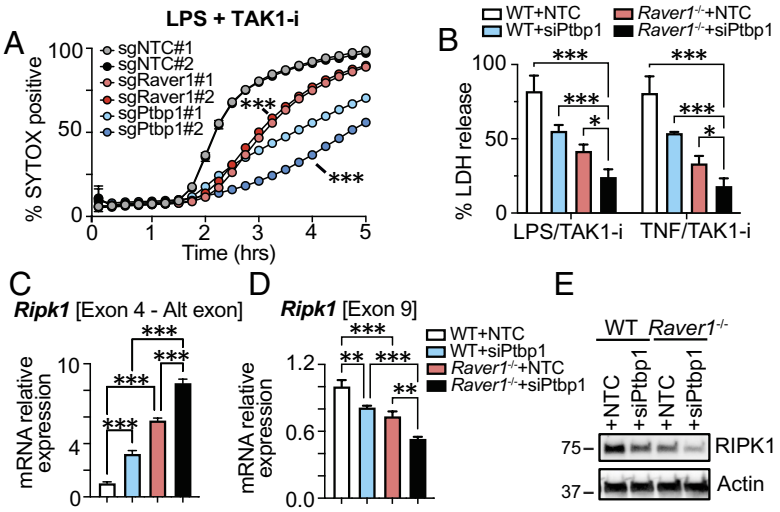

Fig. 5. Raver1 cooperates with Ptbp1 to regulate RIPK1 splicing and cell death. (*A*) Cas9-expressing BMDMs transduced with sgRNA targeting *Raver1* or *Ptbp1* were treated with LPS plus TAK1-i and cell death was measured by SYTOX assay. (*B–E*) WT or *Raver1*$^{-/-}$ immortalized macrophages were transfected with *Ptbp1*-targeting siRNA or NTC siRNA. Cell death was measured by LDH release 4 h after LPS+TAK1-i or TNF+TAK1-i treatment (*B*). qRT-PCR of mRNA levels of *Ripk1* exons normalized to *Actin* (*C* and *D*). Protein levels of RIPK1 were analyzed by immunoblotting (*E*). Data are presented as the mean ± SD for triplicate wells from three or more independent experiments. Immunoblots are representative of three blots performed. For comparison, ANOVA was used with Bonferroni's post hoc test. *$P \le 0.05$, **$P \le 0.01$, ***$P \le 0.001$. Abbreviations: Alt exon, alternative exon.

Fig. S8*C*). Consistently, TDB-induced Mincle expression is substantially reduced in the absence of RIPK1 kinase activity (Fig. 6*H*). Therefore, we propose that Raver1 modulation of RIPK1 impacts Mincle signaling.

Raver1 Is Indispensable for Host Defense against *Yersinia* Infection. To investigate the biological significance of Raver1 in host defenses in vivo, we infected *Raver1*$^{-/-}$ mice orally with *Y. pseudotuberculosis*. Caspase-8 and RIPK1 kinase play central

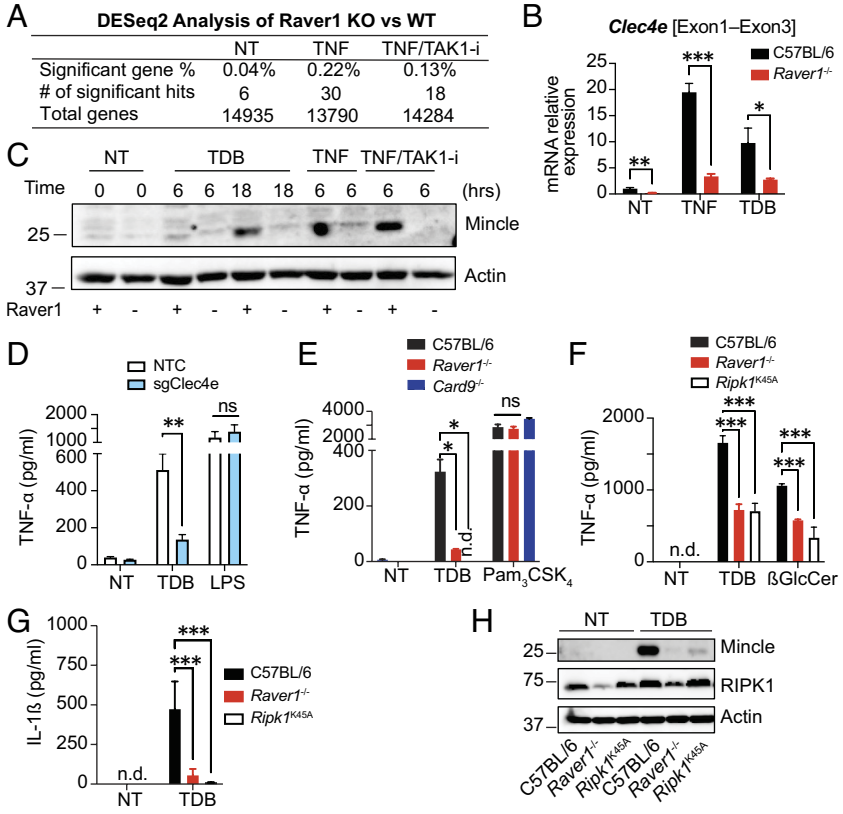

Fig. 6. Raver1 modulates Mincle-dependent TNF release via RIPK1. (*A*) WT or *Raver1*$^{-/-}$ BMDMs were unstimulated (NT) or stimulated for 1 h with TNF or TNF plus TAK1-i and analyzed by RNAseq. Genes with significant differences in expression between WT and *Raver1*$^{-/-}$ are enumerated. (*B* and *C*) WT or *Raver1*$^{-/-}$ BMDMs were stimulated with TNF or synthetic mycobacterial cord factor, trehalose-6,6′-dibehenate (TDB). (*B*) Relative mRNA expression of Mincle (*Clec4e*) was quantified by qRT-PCR after 1-h TNF or 6-h TDB treatment, normalized to *Actin*. (*C*) Protein lysates were analyzed for Mincle level by immunoblotting at the indicated times. (*D–G*) BMDMs transduced with *Clec4e* sgRNA (*D*) or from indicated genotypes (*E–G*) were stimulated with TDB, LPS, Pam_3CSK_4, or cell-death-related β-glucosylceramide (βGlcCer) for 24 h. TNF-α or IL-1β release was assessed by the ELISA. (*H*) WT, *Raver1*$^{-/-}$, and *Ripk1*^{K45A} BMDMs were treated with TDB for 18 h and analyzed by immunoblotting. Data are presented as the mean ± SD for triplicate wells from three or more independent experiments. Immunoblots are representative of three blots performed. For comparison between two groups, Student's *t* test was used; for more than two groups, ANOVA was used with Bonferroni's post hoc test. n.s., not significant; *$P \le 0.05$; **$P \le 0.01$; ***$P \le 0.001$.

roles in host resistance to this gastroenteric pathogen (*SI Appendix*, Fig. S9 *A* and *B*) (13, 14, 46). Compared to C57Bl/6 (*Raver1*$^{+/+}$) or *Raver1*$^{+/-}$ littermates, *Raver1*$^{-/-}$ mice had markedly elevated susceptibility to bacterial challenge (Fig. 7*A*), although the gross composition of immune cells in the spleens was preserved (*SI Appendix*, Fig. S9*C*). Compared to WT mice, bacterial loads

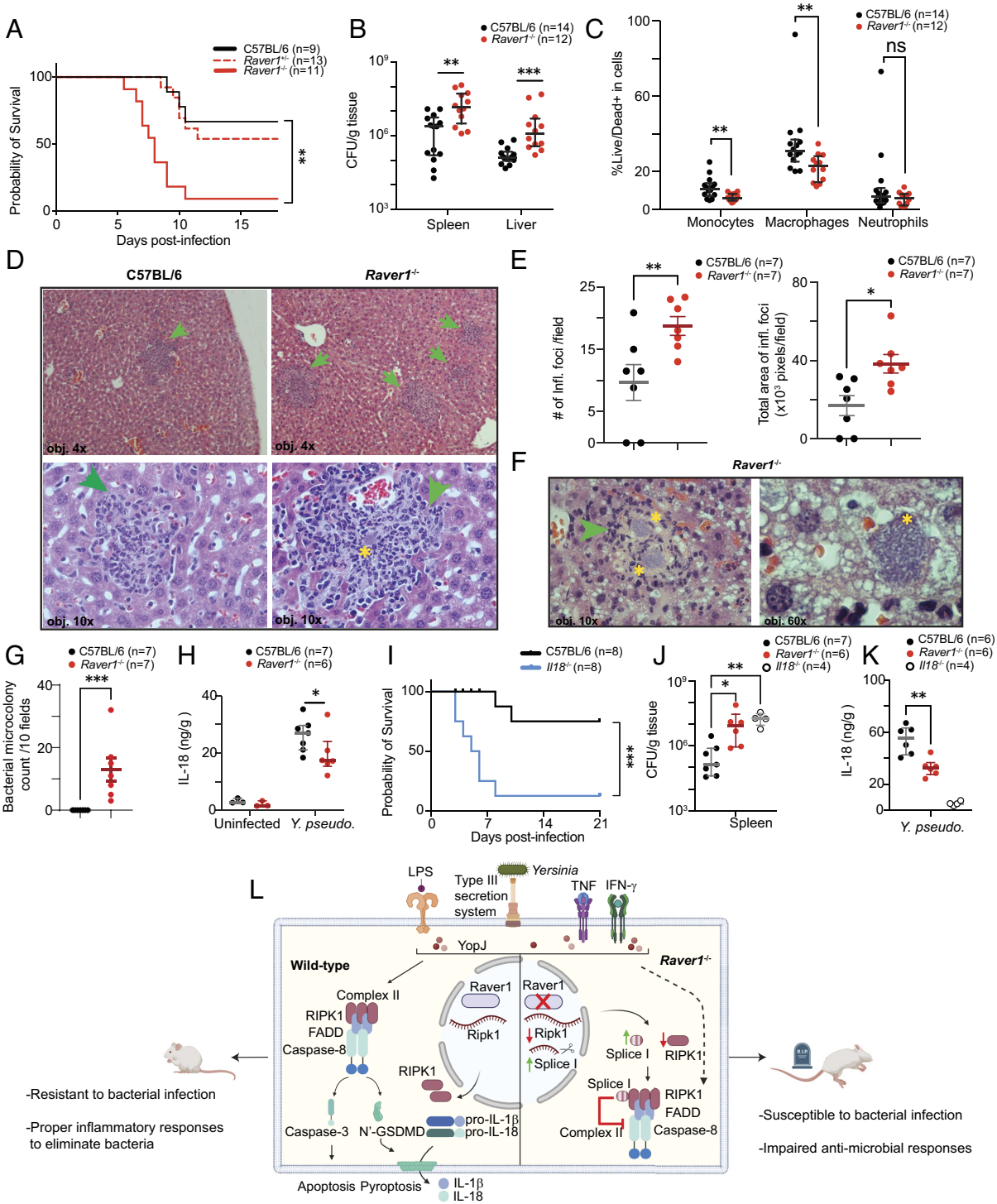

Fig. 7. Raver1 is essential for host resistance against *Y. pseudotuberculosis* infection in vivo. (*A*) Survival of C57BL/6, *Raver1*$^{-/-}$, or heterozygous littermates were monitored following oral challenge with 0.5 to 1 × 10^8 CFU of *Y. pseudotuberculosis*. (*B* and *C*) Tissues from C57BL/6 and *Raver1*$^{-/-}$ mice were collected 5 d postinfection to quantify the bacterial load in spleens and livers (*B*) and analyze subpopulations of CD11b$^+$ myeloid cells in spleens for cell death with live/dead stain by flow cytometry (*C*). (*D*–*G*) Liver sections from C57BL/6 and *Raver1*$^{-/-}$ mice were stained with hematoxylin and eosin and subjected to microscopy. (*D*) Inflammatory foci (green arrows) and (*F*) bacterial microcolonies (yellow asterisks) were quantified (*E* and *G*). Magnification: 40× (4× objective, as indicated), 100× (10× objective), or 600× (60× objective). (*H*) IL-18 in C57BL/6 and *Raver1*$^{-/-}$ mice spleen homogenates 3 d postinfection were measured by the ELISA. (*I*) Survival of C57BL/6 and *Il18*$^{-/-}$ mice challenged orally with 1 × 10^8 CFU of *Y. pseudotuberculosis*. (*J*) Bacterial loads in indicated spleens and (*K*) IL-18 in indicated spleen homogenates were measured by the ELISA 3 d postinfection. Data are presented as medians with interquartile range (*B*, *C*, *H*, *J*, and *K*) or mean with SEM (*E* and *G*), either pooled from two independent experiments (*A*–*C*) or representative of two or more independent experiments (*D*–*K*). Images are representative of two individual experiments. For comparisons, datasets were analyzed by the log-rank test (*A* and *I*), Mann–Whitney *U* test (*B*, *C*, *E*, *G*, *H*, and *K*), or Kruskal–Wallis with Dunn's post hoc test (*J*). *$P \le 0.05$, **$P \le 0.01$, ***$P \le 0.001$. (*L*) Proposed model for Raver1-mediated caspase-8-dependent pyroptotic cell death, inflammation, and pathogen resistance.

in the spleens and livers of *Raver1*$^{-/-}$ mice increased significantly (Fig. 7*B*). Our experiments with BMDMs suggested that Raver1 has a major effect on *Yersinia*-induced cell death (Fig. 2). Consistent with this, we also observed a significant decrease in cytotoxicity in monocytes and macrophages isolated from infected *Raver1*$^{-/-}$ mice (Fig. 7*C* and *SI Appendix*, Fig. S9*D*). Histological analysis of liver tissue showed that increased bacterial loads correlated with increased number and size of inflammatory foci (Fig. 7 *D* and *E*). Notably, visible bacterial microcolonies were observed only in *Raver1*$^{-/-}$ but not in C57Bl/6 mice (Fig. 7 *F* and *G*), indicating that *Raver1*$^{-/-}$ mice had a diminished ability to contain bacterial spread and replication. Therefore, recruited inflammatory cells in *Raver1*$^{-/-}$ livers may not display an appropriate antibacterial capacity, as we have proposed by observing livers from mice with other defects in innate immune signaling (29). Moreover, IL-18 protein levels were markedly downregulated in spleens from *Raver1*$^{-/-}$ mice (Fig. 7*H*), although IL-1ß, TNF, and IL-6 were not significantly changed (*SI Appendix*, Fig. S9 *E–G*). IL-18 is critical for host resistance to *Yersinia* (29, 31, 47). Specifically, we found that genetic ablation of *Il18* resulted in heightened susceptibility to *Y. pseudotuberculosis* gastrointestinal infection (Fig. 7*I*), following increased bacteria load in spleens (Fig. 7*J*), emphasizing the importance of normal IL-18 production in host defenses to this pathogen. Our results indicate that Raver1 regulates *Yersinia*-induced IL-18 production both in vivo (Fig. 7*K*) and in macrophages in vitro (Fig. 3*J*), and the evidence indicates that the Raver1–RIPK1–caspase-8–IL-18 axis is a key contributor to host defenses. We also noticed a small but significant decrease in the percentage of CD69$^+$ B and CD4$^+$ T cell populations in *Yersinia*-infected *Raver1*$^{-/-}$ mice (*SI Appendix*, Fig. S9 *H–J*), suggesting that Raver1 contributes to adaptive immune responses. This is likely a consequence of positive regulation of early innate immune responses to bacteria, by aiding lymphoid cell activation. Collectively, these findings indicate that Raver1 is critical for resistance to infection and to coordinate an appropriate host response to *Yersinia.*

Discussion

Alternative splicing is critical for modulating inflammation and cell death responses by influencing isoform expression of key factors. Here, we identified Raver1 as a crucial upstream regulator of RIPK1-caspase-8-mediated pyroptosis and IL-1ß/IL-18 secretion, uncovering a regulatory mechanism in the interplay between immune responses and cell death pathways. Our data support a role for Raver1 in maintaining RIPK1 abundance and function by repressing the inclusion of an alternative exon during pre-mRNA splicing. We provide evidence that Raver1 regulates innate immunity and cell death in primary macrophages and neutrophils, and in vivo (Fig. 7*L*).

Our data suggest that Raver1 is a pivotal regulator, orchestrating multiple interconnected pathways. In addition to a profound effect on pyroptotic/apoptotic cell death and inflammatory responses (IL-18/IL-1ß release) to *Yersinia* bacteria and the type III secretion system effector molecule YopJ, we also found that Raver1 positively influenced caspase-8-mediated signaling induced by LPS, TNF family members, and IFNγ, and restrained by kinases TAK1 and IKK. In contrast, canonical caspase-1-dependent pyroptosis and IL-1ß/IL-18 release, and raptinal-induced intrinsic apoptosis were unaffected by Raver1. Moreover, Raver1 facilitates MLKL-dependent necroptosis unleashed by caspase-8 blockade, influencing the plasticity between cell death pathways through RIPK1 (48, 49).

Raver1 is ubiquitously expressed in cells and tissues, and its promoter region contains a negative regulator that could be influenced by NF-κB (50). This supports our observations of decreased *Raver1* transcription upon TLR4 stimulation and the presence of a proposed negative feedback loop. Raver1 impacts cell death and inflammation across various cell types, including macrophages, neutrophils, osteosarcoma cells, and fibroblast cells, suggesting that Raver1 plays a fundamental role in coordinating immune responses throughout the body in pathological conditions via its regulation of RIPK1. Additionally, the regulatory role of Raver1 spans species, governing cell death processes in both mouse and human cells. This versatile function underscores its potential significance as a key regulator in cellular homeostasis and immune responses.

Here, we determined that alternative splicing is an important layer of regulation on RIPK1 function in addition to well-established posttranslational modifications. Alternative splicing profoundly impacts the balance between cell survival and death. By altering splicing patterns, cells modulate the expression levels or activities of cell death or survival factors. For example, alternative splicing generates splice variants that either promote or inhibit apoptosis. These variants may possess different protein domains. For example, different splice variants of *cflar* (cFlip) and *bcl-x* can either induce or protect cells from death (12, 51, 52). The RIPK1 Splice I variant is incapable of inducing cell death by itself, as it lacks a significant portion of the RIPK1 protein. Interestingly, we found Splice I directly interacted with full-length RIPK1 and attenuated its activation in a dominant-negative manner, potentially by blocking phosphorylation at S166. Mechanistically, we speculate that Splice I binding to RIPK1 restrains RIPK1 kinase-dependent recruitment of FADD and caspase-8, thus impeding complex II assembly, which is limited in *Raver1*$^{-/-}$ macrophages. Our data revealed reduced newly synthesized but not preexisting RIPK1 protein in the presence of Splice I. One possible explanation is that the absence of *Raver1* and altered splicing could mediate the mRNA decay of steady-state *Ripk1*. Together, the reduction in full-length RIPK1 expression along with the dominant-negative effect of RIPK1 nonfunctional variant Splice I, explain the decrease of pyroptosis/apoptosis in *Raver1*$^{-/-}$ cells during TAK1 inhibition.

Raver1 has been proposed as a regulatory factor of Ptbp1, yet not many Raver1 targets have been identified. While Ptbp1 has a significant impact on a wide range of splicing events from regulation of neuronal differentiation to lymphocyte maturation and activation (22, 53–56), the specific contribution of Raver1 to innate immune function remains largely unexplored. Here, we conclude that Raver 1 modulates signaling induced by both pathogens and cytokines in primary macrophages and mice. This indicates a previously unknown and broad impact on innate immune responses, in part due to alternative splicing regulation. Transcriptomic analyses revealed that loss of Raver1 resulted in few perturbations to mRNA levels, but a widespread effect on transcript composition. We show here that Raver1 influences mRNA isoform diversity primarily through repression of alternative exon inclusion. We also demonstrated that regulation of transcript composition in targets, such as *Ripk1*, has direct effects on physiologically relevant innate immune processes. Further analysis could identify additional immune-related target transcripts of Raver1 and the potential involvement of Ptbp1. These two splicing factors can function together to regulate the splicing of certain genes (19, 20), while Ptbp1-independent alternative splicing by Raver1 is also possible (37). Our data suggest that Raver1 may work in concert with Ptbp1 in regulating *Ripk1* pre-mRNA splicing and subsequent cytotoxicity, as evidenced by the additive effect of modulating Raver1 and Ptbp1. Additional studies are needed to more precisely define the interplay between Ptbp1 and Raver1 during innate immune signaling. We speculate that Raver1 provides further specificity to the action of Ptbp1. Raver1 was proposed to bridge multiple Ptbp1 molecules bound

to polypyrimidine tracts flanking exons to promote RNA looping and splicing repression (21). One possible model is that Raver1 serves as a connection between Ptbp1 proteins flanking the *Ripk1* alternative exon to collaboratively promote its skipping.

Interestingly, we found the expression and function of the CLR Mincle (*Clec4e*) were also impaired in *Raver1*$^{-/-}$ macrophages, although we did not detect a direct link to the splicing of *Clec4e*. Here, we provide evidence that Raver1 controls Mincle via RIPK1 kinase activity. Notably, Dectin-1 (*Clec7a*) has been proposed to relay necroptosis signals via RIPK1, and an interaction with RIPK1 and the CARD9 protein, which also contributes to Mincle signaling, was proposed in macrophages (45). It is possible that Mincle-driven CARD9 serves as an adaptor for RIPK1 binding and activation, controlling downstream NF-κB-activated transcription of proinflammatory cytokines and Mincle (*Clec4e*). This could potentially serve as a feed-forward loop to enhance immunity against infection.

Here, we demonstrate the pathophysiological significance of proper *Ripk1* splicing by Raver1 in the context of *Yersinia* challenge. *Raver1* deficiency decreased inflammatory cytokine release, reduced cell death of host phagocytes, and increased bacterial propagation, culminating in decreased host survival. Surprisingly, we observed a significant decrease in splenic IL-18 but not IL-1ß. This finding may be explained by cytokine upregulation influenced by intensified bacterial burden, and the impact of different caspases contributing to the maturation of IL-18 and IL-1ß under different experimental conditions (57). In this context, a recent study proposed that IL-1ß is less important for mouse survival against *Y. pseudotuberculosis* infection (58), whereas our experiments show that IL-18 is a strong positive factor in host defenses. Our findings indicate that Raver1 may not primarily influence the recruitment of phagocytes to infected sites, but rather is essential for their effective antibacterial functions. In addition, we noted a significant proportional decrease in activated CD69^{+} spleen T and B cells upon deletion of *Raver1*, indicative of a potential impact on adaptive immune responses. Regulation of IL-18 production may also influence adaptive immune responses. Raver1 may contribute to lymphocyte priming through IL-18 regulation, thereby assisting adaptive immunity.

Yersinia infections are an excellent model to study the RIPK1–caspase-8–GSDMD axis with potential implications in different immune contexts. RIPK1 contributes to many diseases, including bacterial infection (46), dermatitis (59), autoinflammatory diseases (60, 61), cancer (3), and neuroinflammation (62). Additionally, a link between caspase-8 and GSDMD has been proposed for intestinal inflammation triggered by mutation of FADD (63). These intersecting crosstalk pathways are prime targets for drug development. Decreased expression of TAK1 in the aging process has also been implicated in neuroinflammation (64), and TAK1 inhibition is being tested for cancer therapy (65, 66). Thus, our signaling studies are relevant for pathological conditions beyond bacterial infection. Interestingly, a recent study identified three cases of patients carrying homozygous mutations in RIPK1 causing recurrent infections and severe inflammatory dysregulation (67). These mutations resulted in a premature stop codon within the RIPK1 kinase domain, producing truncated proteins, much like Splice I in Raver1-deficient conditions. Moreover, genome-wide association studies have suggested that SNPs within the *RAVER1* locus are associated with COVID-19 disease severity and also inflammatory diseases (68, 69), indicating that regulation of Raver1 could impact both infectious and sterile inflammatory conditions. Taken together, our data elucidate a layer of *Ripk1* splicing regulation and could aid the development of therapeutic strategies to control and fine-tune inflammatory responses.

Materials and Methods

Mice and Bacterial Strains. Experiments involving mice were approved by the UMass Chan Institutional Animal Care and Use Committee. Most mouse strains were described previously (13, 15, 29, 30). *Raver1*$^{-/-}$ mice were generated in-house in this study. *Y. pestis*, *Y. pseudotuberculosis*, *Y. enterocolitica*, their derivative strains, and *S. enterica* serovar Typhimurium, were used as previously described (13, 15, 31). See *SI Appendix, SI Materials and Methods*.

Cell Culture. BMDMs were differentiated from bone marrow harvested from femurs and tibia, as described (30, 31). See *SI Appendix, SI Materials and Methods*.

CRISPR Cell Death Screens. Forward genetic genome-wide screens were performed using the mouse BRIE knockout CRISPR pooled library designed by David Root and John Doench (70) (Addgene 73633) in Cas9-expressing BMDMs. See *SI Appendix, SI Materials and Methods*.

Data, Materials, and Software Availability. The raw data files of sequencing experiments have been deposited in the National Center for Biotechnology Information Gene Expression Omnibus database. The accession number is GEO: GSE281137 (71). All data needed to evaluate the conclusions in this paper are present either in the main text or in *SI Appendix*.

ACKNOWLEDGMENTS. The UMass Chan Medical School Transgenic Animal Modeling Core is acknowledged for assistance with generation of *Raver1*$^{-/-}$ animals. We thank C. Choquette and Z. Jiang for help with mice, M. Trombly for assistance with manuscript development, V. Boyartchuk for discussions, E. Pearlman for advice on neutrophil experiments, and A. Olive, C. Sassetti, P. Meraner, and A. Brass for input on CRISPR screen methods. Funding: The work was funded by NIH grants AI075318, AI129527, AI159706, AI181309 (E.L.), AI067497, AI083713 (K.A.F.), AI075811 (M.A.K.), GM133762 (A.A.P.), and a diversity supplement to GM133762 (L.T.-U.), AI095213 (A.D.). Additional funding was provided by The Norwegian Cancer Society B05035/001 (E.L.) and the Research Council of Norway, Center of Excellence Funding Scheme project 223255/F50 (P.O., L.R., T.E., K.A.F., and E.L.).

Author affiliations: [a]Division of Infectious Diseases and Immunology, Department of Medicine, Program in Innate Immunity, University of Massachusetts Chan Medical School, Worcester, MA 01605; [b]Department of Clinical and Molecular Medicine, Centre of Molecular Inflammation Research, Norwegian University of Science and Technology, Trondheim 7491, Norway; [c]RNA Therapeutics Institute, University of Massachusetts Chan Medical School, Worcester, MA 01655; [d]Institute for Immunodeficiency, Center of Chronic Immunodeficiency, University Medical Center, Faculty of Medicine, University of Freiburg, Freiburg 79106, Germany; [e]Institute for Immunodeficiency, Center for Pediatrics and Adolescent Medicine University Medical Center, Faculty of Medicine, University of Freiburg, Freiburg 79106, Germany; [f]Department of Molecular Cell and Cancer Biology, University of Massachusetts Chan Medical School, Worcester, MA 01605; [g]Pattern Recognition Receptor Discovery Performance Unit, Immuno-Inflammation Therapeutic Area, GlaxoSmithKline, Collegeville, PA 19426; [h]Sanofi, Immunology and Inflammation Research Therapeutic Area, Cambridge, MA 02141; [i]Department of Microbiology and Physiological Systems, University of Massachusetts Chan Medical School, Worcester, MA 01655; [j]Department of Laboratory Medicine and Pathology, Center for Individualized Medicine, Mayo Clinic, Rochester, MN 55905; [k]Clinic of Laboratory Medicine, St. Olavs Hospital, Trondheim 7006, Norway; and [l]Division of Innate Immunity, Department of Medicine, University of Massachusetts Chan Medical School, Worcester, MA 01605

Author contributions: B.Z., P.O., K.A.F., and E.L. conceptualized the study; B.Z., P.O., A.D., and R.E. performed investigation; J.B., M.K.P., J.D.G., L.R., and T.E. contributed new reagents; B.Z., J.W.L., L.T.-U., M.A.K., R.K.K., T.E., and A.A.P. discussed the data; B.Z., J.W.L., L.T.-U., M.A.K., R.K.K., T.E., and A.A.P. analyzed the data; M.A.K., R.K.K., T.E., A.A.P., K.A.F., and E.L. acquired funding; A.A.P., K.A.F., and E.L. supervised the study; B.Z., P.O., and E.L. wrote the original draft; and all authors wrote, reviewed, and edited the paper.

1. B. Tummers, D. R. Green, Caspase-8: Regulating life and death. *Immunol. Rev.* **277**, 76–89 (2017).
2. P. Orning, E. Lien, Multiple roles of caspase-8 in cell death, inflammation, and innate immunity. *J. Leukoc. Biol.* **109**, 121–141 (2021).
3. J. Clucas, P. Meier, Roles of RIPK1 as a stress sentinel coordinating cell survival and immunogenic cell death. *Nat. Rev. Mol. Cell Biol.* **24**, 835–852 (2023).
4. N. Paquette *et al.*, Serine/threonine acetylation of TGFbeta-activated kinase (TAK1) by Yersinia pestis YopJ inhibits innate immune signaling. *Proc. Natl. Acad. Sci. U.S.A.* **109**, 12710–12715 (2012).

5. U. Meinzer *et al.*, Yersinia pseudotuberculosis effector YopJ subverts the Nod2/RICK/TAK1 pathway and activates caspase-1 to induce intestinal barrier dysfunction. *Cell Host Microbe* **11**, 337–351 (2012).
6. S. Mukherjee *et al.*, Yersinia YopJ acetylates and inhibits kinase activation by blocking phosphorylation. *Science* **312**, 1211–1214 (2006).
7. R. Mittal, S. Y. Peak-Chew, H. T. McMahon, Acetylation of MEK2 and I kappa B kinase (IKK) activation loop residues by YopJ inhibits signaling. *Proc. Natl. Acad. Sci. U.S.A.* **103**, 18574–18579 (2006).
8. R. K. S. Malireddi *et al.*, TAK1 restricts spontaneous NLRP3 activation and cell death to control myeloid proliferation. *J. Exp. Med.* **215**, 1023–1034 (2018).
9. K. Maeda, J. Nakayama, S. Taki, H. Sanjo, TAK1 limits death receptor fas-induced proinflammatory cell death in macrophages. *J. Immunol.* **209**, 1173–1179 (2022).
10. Y. Dondelinger *et al.*, NF-kappaB-independent role of IKKalpha/IKKbeta in preventing RIPK1 kinase-dependent apoptotic and necroptotic cell death during TNF signaling. *Mol. Cell* **60**, 63–76 (2015).
11. Y. Dondelinger *et al.*, Serine 25 phosphorylation inhibits RIPK1 kinase-dependent cell death in models of infection and inflammation. *Nat. Commun.* **10**, 1729 (2019).
12. H. I. Muendlein *et al.*, cFLIP(L) protects macrophages from LPS-induced pyroptosis via inhibition of complex II formation. *Science* **367**, 1379–1384 (2020).
13. D. Weng *et al.*, Caspase-8 and RIP kinases regulate bacteria-induced innate immune responses and cell death. *Proc. Natl. Acad. Sci. U.S.A.* **111**, 7391–7396 (2014).
14. N. H. Philip *et al.*, Caspase-8 mediates caspase-1 processing and innate immune defense in response to bacterial blockade of NF-kappaB and MAPK signaling. *Proc. Natl. Acad. Sci. U.S.A.* **111**, 7385–7390 (2014).
15. P. Orning *et al.*, Pathogen blockade of TAK1 triggers caspase-8-dependent cleavage of gasdermin D and cell death. *Science* **362**, 1064–1069 (2018).
16. S. B. Kovacs, E. A. Miao, Gasdermins: Effectors of pyroptosis. *Trends Cell Biol.* **27**, 673–684 (2017).
17. J. Sarhan *et al.*, Caspase-8 induces cleavage of gasdermin D to elicit pyroptosis during Yersinia infection. *Proc. Natl. Acad. Sci. U.S.A.* **115**, E10888–E10897 (2018).
18. Z. Zheng *et al.*, The lysosomal Rag-ragulator complex licenses RIPK1 and caspase-8-mediated pyroptosis by Yersinia. *Science* **372**, eabg0269 (2021).
19. S. Huttelmaier *et al.*, Raver1, a dual compartment protein, is a ligand for PTB/hnRNPI and microfilament attachment proteins. *J. Cell Biol.* **155**, 775–786 (2001).
20. N. Gromak *et al.*, The PTB interacting protein raver1 regulates alpha-tropomyosin alternative splicing. *EMBO J.* **22**, 6356–6364 (2003).
21. A. P. Rideau *et al.*, A peptide motif in Raver1 mediates splicing repression by interaction with the PTB RRM2 domain. *Nat. Struct. Mol. Biol.* **13**, 839–848 (2006).
22. N. Keppetipola, S. Sharma, Q. Li, D. L. Black, Neuronal regulation of pre-mRNA splicing by polypyrimidine tract binding proteins, PTBP1 and PTBP2. *Crit. Rev. Biochem. Mol. Biol.* **47**, 360–378 (2012).
23. Y. Zhao *et al.*, The NLRC4 inflammasome receptors for bacterial flagellin and type III secretion apparatus. *Nature* **477**, 596–600 (2011).
24. M. G. Callow *et al.*, CRISPR whole-genome screening identifies new necroptosis regulators and RIPK1 alternative splicing. *Cell Death Dis.* **9**, 261 (2018).
25. R. K. S. Malireddi *et al.*, Whole-genome CRISPR screen identifies RAVER1 as a key regulator of RIPK1-mediated inflammatory cell death, PANoptosis. *iScience* **26**, 106938 (2023).
26. K. W. Chen *et al.*, RIPK1 activates distinct gasdermins in macrophages and neutrophils upon pathogen blockade of innate immune signaling. *Proc. Natl. Acad. Sci. U.S.A.* **118**, e2101189118 (2021).
27. L. Laurien *et al.*, Autophosphorylation at serine 166 regulates RIP kinase 1-mediated cell death and inflammation. *Nat. Commun.* **11**, 1747 (2020).
28. A. Polykratis *et al.*, Cutting edge: RIPK1 Kinase inactive mice are viable and protected from TNF-induced necroptosis in vivo. *J. Immunol.* **193**, 1539–1543 (2014).
29. G. I. Vladimer *et al.*, The NLRP12 inflammasome recognizes Yersinia pestis. *Immunity* **37**, 96–107 (2012).
30. D. Ratner *et al.*, The Yersinia pestis effector YopM inhibits pyrin inflammasome activation. *PLoS Pathog.* **12**, e1006035 (2016).
31. D. Ratner *et al.*, Manipulation of interleukin-1beta and interleukin-18 production by Yersinia pestis effectors YopJ and YopM and redundant impact on virulence. *J. Biol. Chem.* **291**, 9894–9905 (2016).
32. Y. Zheng *et al.*, A Yersinia effector with enhanced inhibitory activity on the NF-kappaB pathway activates the NLRP3/ASC/caspase-1 inflammasome in macrophages. *PLoS Pathog.* **7**, e1002026 (2011).
33. F. R. Greten *et al.*, NF-kappaB is a negative regulator of IL-1beta secretion as revealed by genetic and pharmacological inhibition of IKKbeta. *Cell* **130**, 918–931 (2007).
34. R. Karki *et al.*, Synergism of TNF-alpha and IFN-gamma triggers inflammatory cell death, tissue damage, and mortality in SARS-CoV-2 infection and cytokine shock syndromes. *Cell* **184**, 149–168. e17 (2021).
35. D. S. Simpson *et al.*, Interferon-gamma primes macrophages for pathogen ligand-induced killing via a caspase-8 and mitochondrial cell death pathway. *Immunity* **55**, 423–441.e9 (2022).
36. T. Espevik, J. Nissen-Meyer, A highly sensitive cell line, WEHI 164 clone 13, for measuring cytotoxic factor/tumor necrosis factor from human monocytes. *J. Immunol. Methods* **95**, 99–105 (1986).
37. A. Wedler *et al.*, RAVER1 hinders lethal EMT and modulates miR/RISC activity by the control of alternative splicing. *Nucleic Acids Res.* **52**, 3971–3988 (2024), 10.1093/nar/gkae046.
38. E. Meylan *et al.*, RIP1 is an essential mediator of Toll-like receptor 3-induced NF-kappa B activation. *Nat. Immunol.* **5**, 503–507 (2004).
39. H. Chen *et al.*, RAVER1 is a coactivator of MDA5-mediated cellular antiviral response. *J. Mol. Cell Biol.* **5**, 111–119 (2013).
40. L. Gitlin *et al.*, Essential role of mda-5 in type I IFN responses to polyriboinosinic:Polyribocytidylic acid and encephalomyocarditis picornavirus. *Proc. Natl. Acad. Sci. U.S.A.* **103**, 8459–8464 (2006).
41. J. Schick *et al.*, Cutting edge: TNF is essential for mycobacteria-induced MINCLE expression, macrophage activation, and Th17 adjuvanticity. *J. Immunol.* **205**, 323–328 (2020).
42. E. C. Patin, S. J. Orr, U. E. Schaible, Macrophage inducible C-type lectin as a multifunctional player in immunity. *Front. Immunol.* **8**, 861 (2017).
43. H. Schoenen *et al.*, Cutting edge: Mincle is essential for recognition and adjuvanticity of the mycobacterial cord factor and its synthetic analog trehalose-dibehenate. *J. Immunol.* **184**, 2756–2760 (2010).
44. M. Nagata *et al.*, Intracellular metabolite beta-glucosylceramide is an endogenous Mincle ligand possessing immunostimulatory activity. *Proc. Natl. Acad. Sci. U.S.A.* **114**, E3285–E3294 (2017).
45. M. Cao *et al.*, Dectin-1-induced RIPK1 and RIPK3 activation protects host against Candida albicans infection. *Cell Death Differ.* **26**, 2622–2636 (2019).
46. L. W. Peterson *et al.*, RIPK1-dependent apoptosis bypasses pathogen blockade of innate signaling to promote immune defense. *J. Exp. Med.* **214**, 3171–3182 (2017).
47. E. Bohn *et al.*, IL-18 (IFN-gamma-inducing factor) regulates early cytokine production in, and promotes resolution of, bacterial infection in mice. *J. Immunol.* **160**, 299–307 (1998).
48. K. Newton *et al.*, Activity of caspase-8 determines plasticity between cell death pathways. *Nature* **575**, 679–682 (2019).
49. M. Fritsch *et al.*, Caspase-8 is the molecular switch for apoptosis, necroptosis and pyroptosis. *Nature* **575**, 683–687 (2019).
50. M. G. Romanelli, P. Lorenzi, F. Avesani, C. Morandi, Functional characterization of the ribonucleoprotein, PTB-binding 1/Raver1 promoter region. *Gene* **405**, 79–87 (2007).
51. D. R. Ram *et al.*, Balance between short and long isoforms of cFLIP regulates Fas-mediated apoptosis in vivo. *Proc. Natl. Acad. Sci. U.S.A.* **113**, 1606–1611 (2016).
52. C. F. A. Warren, M. W. Wong-Brown, N. A. Bowden, BCL-2 family isoforms in apoptosis and cancer. *Cell Death Dis.* **10**, 177 (2019).
53. E. Monzon-Casanova *et al.*, The RNA-binding protein PTBP1 is necessary for B cell selection in germinal centers. *Nat. Immunol.* **19**, 267–278 (2018).
54. J. La Porta, R. Matus-Nicodemos, A. Valentin-Acevedo, L. R. Covey, The RNA-binding protein, polypyrimidine tract-binding protein 1 (PTBP1) is a key regulator of CD4 T cell activation. *PLoS One* **11**, e0158708 (2016).
55. S. Vavassori, Y. Shi, C. C. Chen, Y. Ron, L. R. Covey, In vivo post-transcriptional regulation of CD154 in mouse CD4+ T cells *Eur. J. Immunol.* **39**, 2224–2232 (2009).
56. J. A. Hensel *et al.*, Splice factor polypyrimidine tract-binding protein 1 (Ptbp1) primes endothelial inflammation in atherogenic disturbed flow conditions. *Proc. Natl. Acad. Sci. U.S.A.* **119**, e2122227119 (2022).
57. B. Demarco *et al.*, Caspase-8-dependent gasdermin D cleavage promotes antimicrobial defense but confers susceptibility to TNF-induced lethality. *Sci. Adv.* **6**, eabc3465 (2020).
58. R. Matsuda *et al.*, A TNF–IL-1 circuit controls Yersinia within intestinal pyogranulomas. *J. Exp. Med.* **221**, e20230679 (2024).
59. S. B. Berger *et al.*, Cutting Edge: RIP1 kinase activity is dispensable for normal development but is a key regulator of inflammation in SHARPIN-deficient mice. *J. Immunol.* **192**, 5476–5480 (2014).
60. N. Lalaoui *et al.*, Mutations that prevent caspase cleavage of RIPK1 cause autoinflammatory disease. *Nature* **577**, 103–108 (2020).
61. P. Tao *et al.*, A dominant autoinflammatory disease caused by non-cleavable variants of RIPK1. *Nature* **577**, 109–114 (2020).
62. L. Mifflin, D. Ofengeim, J. Yuan, Receptor-interacting protein kinase 1 (RIPK1) as a therapeutic target. *Nat. Rev. Drug Discov.* **19**, 553–571 (2020).
63. R. Schwarzer, H. Jiao, L. Wachsmuth, A. Tresch, M. Pasparakis, FADD and caspase-8 Regulate gut homeostasis and inflammation by controlling MLKL- and GSDMD-mediated death of intestinal epithelial cells. *Immunity* **52**, 978–993.e6 (2020).
64. D. Xu *et al.*, TBK1 suppresses RIPK1-driven apoptosis and inflammation during development and in aging. *Cell* **174**, 1477–1491.e19 (2018).
65. R. Santoro, C. Carbone, G. Piro, P. J. Chiao, D. Melisi, TAK-ing aim at chemoresistance: The emerging role of MAP3K7 as a target for cancer therapy. *Drug Resist. Updat.* **33–35**, 36–42 (2017).
66. A. Singh *et al.*, TAK1 inhibition promotes apoptosis in KRAS-dependent colon cancers. *Cell* **148**, 639–650 (2012).
67. D. Cuchet-Lourenco *et al.*, Biallelic RIPK1 mutations in humans cause severe immunodeficiency, arthritis, and intestinal inflammation. *Science* **361**, 810–813 (2018).
68. D. Ellinghaus *et al.*, Analysis of five chronic inflammatory diseases identifies 27 new associations and highlights disease-specific patterns at shared loci. *Nat. Genet.* **48**, 510–518 (2016).
69. I. M. Fink-Baldauf, W. D. Stuart, J. J. Brewington, M. Guo, Y. Maeda, CRISPRi links COVID-19 GWAS loci to LZTFL1 and RAVER1. *EBioMedicine* **75**, 103806 (2022).
70. J. G. Doench *et al.*, Optimized sgRNA design to maximize activity and minimize off-target effects of CRISPR-Cas9. *Nat. Biotechnol.* **34**, 184–191 (2016).
71. B. Zhang, P. Orning, K. A. Fitzgerald, E. Lien, Raver1 links Ripk1 RNA splicing to caspase-8-mediated pyroptotic cell death, inflammation, and pathogen resistance. NCBI Gene Expression Omnibus. https://www.ncbi.nlm.nih.gov/geo/query/acc.cgi?acc=GSE281137. Deposited 23 October 2024.